Simulation and Implementation of an Induction Heating System for Heating Brittle Thin Metal Sheets by Various Excitation Current Frequencies

Gevrek İnce Metal Sacların Çeşitli Uyarma Akımı Frekanslarıyla Isıtmak için İndüksiyonla Isıtma Sisteminin Simülasyonu ve Gerçekleştirilmesi

Sude Hatem [1*] iD

[1]*Faculty of Engineering, Electrical and Electronics Engineering, Çankaya University, 06790 Ankara, Türkiye*

Öz

İndüksiyonla ısıtma işlemi birçok farklı değişkenle ilişkili olduğundan dolayı doğrusal olmayan bir problemdir. Bu problemin matematiksel analizi oldukça zordur ve basitleştirilmesi gerekmektedir. Çoğu durumda, parametrelerin mekansal geometriye dayalı olarak hesaplanması da önem taşımaktadır. Bu çalışma indüksiyonla ısıtma probleminin bir simülasyon modelini ele almaktadır. Arşimet spiral bobininin çeşitli akımları ve frekansları altında kırılgan metal levhaların indüksiyonla ısıtma özellikleri, karmaşık yapılara bir çözüm olan COMSOL Multiphysics'in sonlu elemanlar yöntemi kullanılarak simüle edilmiştir. Kısmi etkileri ayırt etmek için bobin modeli, gerçek bobinin geometrisine çok yakın olacak şekilde ayarlanmıştır. Simülasyon süreci iki aşamadan oluşmaktadır. İlk durum, frekans alanı analizinde uyarma akımı frekansının kademeli olarak arttırılmasıyla ısıtma işleminin değerlendirilmesi ile elde edilirken, ikinci durum, frekans geçici durumunda sabit frekanslı bir akımın uygulanması ve ısıtma işleminin modelde değerlendirilmesi ile elde edilir. Dolayısıyla simülasyon modeli her iki durumda da iş parçası malzemesinin doğrusal olmayan elektromanyetik ve termal özellikleri hakkında temel bilgileri sağlar. Simülasyon modeli sonuçlarını doğrulamak için bir laboratuvar modeli geliştirilip ve deneysel sıcaklık ölçümleri simülasyon sonuçlarıyla karşılaştırılmıştır.

Anahtar Kelimeler

"İndüksiyonla ısıtma, Manyetik akı, Elektromanyetik, Doğrusal Olmama, Multifizik"

Abstract

The induction heating process is a highly nonlinear problem due to its connection with various factors. The complex nature of this issue presents a notable difficulty for mathematical analysis and requires a simplification. Additionally, deriving parameters from spatial geometry can present a notable challenge. This paper deals with a simulation model of the induction heating problem. The finite element method within COMSOL Multiphysics is utilized to simulate the induction heating characteristics of fragile metal sheets subjected to different currents and frequencies from an Archimedean spiral coil. This serves as an effective solution for complex constructions. To differentiate between various influences, the coil model is modified to closely resemble the geometry of the actual coil. The simulation process includes two phases. The first phase involves evaluating the heating process by gradually increasing the frequency in frequency domain analysis and the second phase involves implementing constant frequency current in a frequency transient condition and assessing the heating procedure within the model. Thus, the model provides crucial insights into the nonlinear electromagnetic and thermal properties of the material. To validate the model's results, a laboratory prototype is constructed, and a comparison between experimental temperature measurements and simulation results is performed.

Key Words

Sorumlu Yazar: sudehatem@cankaya.edu.tr

1. Introduction

Recently, methods for induction heating (IH) have seen extensive use in the metallurgical and semiconductor sectors. "Induction heating stands out as a distinctive non-contact method for heating electrically conductive materials. This method, as its name suggests, relies on heating material-induced eddy currents internally. The principal process of heat dissipation caused by Joule's heat is caused by the flow of these eddy currents in electrically conductive materials. Processes such as machining metals (hardening and annealing), pre-deformation heating (forging, extrusion, bending, and drilling), brazing, shrinkage, coating, melting, crystal growth, cap sealing, and carbon vapor deposition widely utilize induction heating as Gholami et al. (2022) and Qu et al. (2013) mention. IH applications vary depending on the frequency employed and system operating frequencies can range from 10 Hz to 900 kHz. Designing an IH system requires understanding the process applied to the workpiece and the induction coil. This encompasses electromagnetic phenomena, including the interplay between the workpiece and the induction coil, uneven distribution of magnetic flux density and current density within both the workpiece and coil, and their respective geometric structures. Other aspects of the induction heating phenomenon to take into account include heat generation, heat transmission inside the material, and heat transfer between the substance and the surrounding environment. The physical characteristics of the substance to be heated is all involved in the aforementioned procedures. These features encompass the electromagnetic and thermal attributes of the material, both of which are significantly impacted by temperature. The quantity of heat generated in the workpiece is contingent on the strength of the electric current flowing through the coil, and the extent of heating are influenced by the frequency of the current.
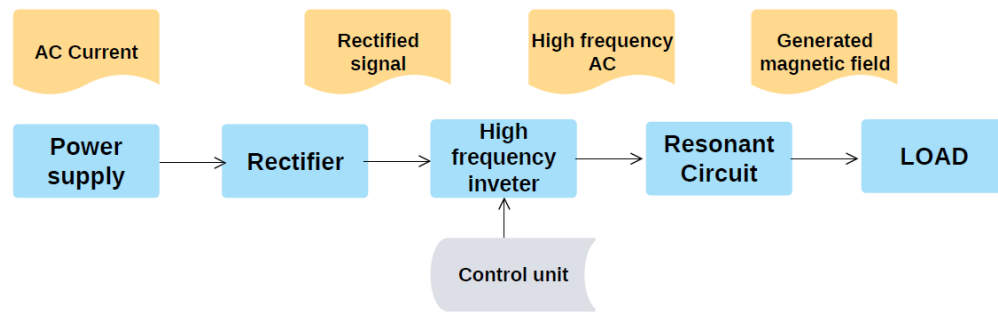

Figure 1. The block diagram of an induction heating system

Given the aforementioned information, the IH phenomenon is a complicated issue; Therefore, numerical simulations seem to be an appropriate tool in the advancement and evaluation of IH systems as Liu & Rao (2009) present. As depicted in Figure 1, the fundamental components of an IH system are an AC source, an induction coil, and the workpiece. To establish the AC source, as discussed by SEGURA (2012), it is essential to determine the equivalent inductance (L_{eq}) and the equivalent resistance (R_{eq}) of coupling between the induction coil and workpiece. This calculation is performed according to either the series or parallel model of coupling. Aflyatunov et al.(2022) established a technological solution for a system of locally associated induction heating of a lengthy pipeline utilizing functional methodologies and presented an induction heating system for an extended pipeline that incorporates the technique of local-associated heating. Brittle materials including aluminum, magnesium, titanium, and nickel alloys are manufactured using an electromagnetic forming and induction heating system that has been established by Baranoğlu et al. (2020). These materials are increasingly used in the transportation, aerospace, and defense industries. As a test of the software's essential correctness, Kennedy et al. (2011) compare the analytical and numerical conclusions for the inductance of a blank "current sheet" inductor.

It also investigates how the calculated total inductance is impacted by the dimensions of the computational space, referred to as the "magnetic domain. The implementation of a brittle metal heating procedure using an electromagnetic field has been suggested by Aydemir et al.(2019). The proposed system is created for a 1 kW power level, and the processes of heat production are thoroughly explored. The design of the heating system, which employs electromagnetic induction heating technology, is addressed by Jinkun et al.(2021). A graphite crucible's induction heating properties have been simulated using COMSOL code with various inductor current and frequency conditions. Considering frequency, it has been feasible to ascertain the connection between the average heat of the crucible and the inductor's current, which is useful for choosing the induction heating system's power source. The procedure of heating a pipe-inductor system for induction welding is described by a model provided by Bocharova et al.(2019). As a distinct structural component of the waveguide path, the framework depicts the induction heating of the pipe. The pipe heating graphs were produced during the software simulation procedure using numerical simulation techniques and the coupling of the appropriate media used in induction heating. The effects of various laser processes and induction heating parameters have been examined by Dalaee et al. (2019) to gather the knowledge needed to create an appropriate IH configuration that can work with the

Direct Metal Deposition (DMD) method. A new heating coil design has been suggested by Miyake et al. (2022). The soft-magnetic cores that protect the coil entrance edges and outer coil perimeter are incorporated into the construction of the suggested heating coils. The results of the investigation have led to the determination that the additional cores can both raise the magnetic field within the heating item, which can raise heat output, and decrease the localized intense magnetic field all around the coil, which can mitigate eddy current induction within the wire and decrease copper loss. An evaluation was performed through simulation to gauge the efficiency of the suggested heating coil configuration. In accordance with the research results, heat generation in the heating item increased by 53% whereas the coil copper loss was reduced by 25%. In the context of internet fusion in research, Dou (2022) explored the mechanism for controlling temperature through electromagnetic induction heating. A proposed method involves a real-time two-way coupling calculation across multiple fields, encompassing electricity, magnetism, heat, and force. Additionally, a numerical approach has been introduced for the computation of these four distinct real-time couplings. The temperature control performance has grown by 10.1%, and the temperature precision has been 96.7%. The development of one induction electric heating method that employed a resonant circuit of zero-voltage switching but not frequently utilized in cooker coils (ZVS) has been addressed by Waluyo et al. (2022). "A common application of induction heating technology is reheating aluminum billets before forging or extruding. As previously stated, the magneto-motive force—the magnetic flux produced by a time-varying current that passes in the induction coil—is what propels the procedure. The present study focuses on the development of an induction heating system and focuses on the induction coil simulation procedures. As Kennedy et al.(2011) and Ludtke &Schulze (2001) mentioned, COMSOL® Multiphysics Software Package, which offers a graphical and interactive simulation environment is used to examine the configuration of induction heating. The associations involving the workpiece and the induction coil that exist during the heating process can be evaluated using the developed model. As a result of their growing utilization in the aerospace sector Al7075 alloy materials are used in the experimental measurements. Section 2 presents the operational principle of the entire system and associated considerations. In section 3 the methodology, equations, and the modeling approach of the proposed coil are investigated.

Section 4 offers an in-depth exposition of the outcomes obtained from the simulation and Section 5 introduces the experimental study and its outcomes. Lastly, in Section 6, the final remarks for the proposed model are provided.

2. Operation Principle of the System and Considerations

The basis of an induction heating system is a resonance circuit made up of a coil and capacitor, a resistor, a rectifier circuit, and an inverter circuit Aydemir et al. (2019). The most optimal and effective approach to transfer energy to the object intended for heating involves the use of resonant circuits. A bridge-type inverter is among the frequently used techniques for producing the high-frequency current needed for induction heating Esteve, (2015). Bridge-type inverters add complexity to the design and are expensive because of the electronic components. However, they offer many benefits, including a wide power control range, high efficiency, and high output power as Najafi &Yatim (2019) imply. Figure 2 depicts the system schematic used in this project. Usually, the AC line voltages are rectified to produce the DC bus voltage. The system functions as a load resonance inverter when a series or parallel capacitor is added to the coil and can be fed by a current or a voltage source. The system's input voltage and current should be determined according to the particular heat, mass, density, magnetic permeability, resistance, and scales of the material to heat a particular workpiece. High-frequency on/off switching of the inverter creates a square wave voltage across the load. This switching frequency is chosen to be close to the resonance frequency. The heat treatment occurs when eddy currents are induced on the metal substrate by the electromagnetic field produced by the resonant current. In practice, the way the coil and workpiece are arranged can be regarded as an electric transformer. The coil serves as the primary, receiving electrical energy, and the workpiece with a short circuit, provides the secondary.
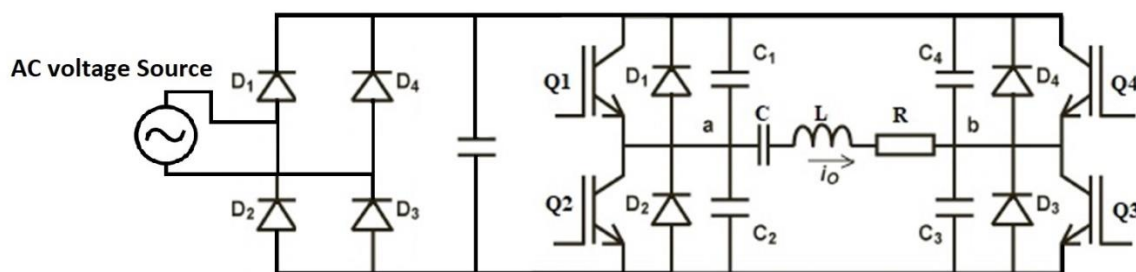

Figure 2. Schematic diagram of circuit

The heating depth in the workpiece and the power transmission rate are both affected by the operational frequency. At the resonant frequency, the impedance reaches its lowest value, allowing the transfer of the highest possible power to the load.

3. Methodology, Equations, and the COMSOL Modeling Approach

3.1. COMSOL Multiphysics

COMSOL Multiphysics is an advanced numerical simulation software developed using finite element analysis. It is adaptable, easy operated, and offers the benefit of conducting multiphysics field coupling analysis as Xiaolong et al. (2011) point to. To present a comparison for experimental performance, a 2D model of the induction heating analysis is generated in this section using the commercial code of COMSOL 5.6® for various operating conditions.

As a starting point, this model quickly resolves Maxwell's equations in the frequency domain using the magnetic vector potential. The problem definition must include the specification of the electromagnetic field:

$$\vec{B} = \vec{\nabla} \times \vec{A} \qquad (1)$$

where $\vec{B}$ [T] gives the flux density and $\vec{A}$ [Wb/m] gives the vector potential.

$$\vec{B} = \mu_0 \mu_r \mu \vec{H} \qquad (2)$$

where $\vec{H}$ [A/m] is the magnetic field intensity.

$$\nabla \times \vec{H} = \vec{J} \qquad (3)$$

where $\vec{J}$ [A/m²] gives the current density and the displacement current $[\frac{\partial D}{\partial t}]$ is neglected.

$$\vec{J} = \sigma \vec{E} + \vec{J_e} \qquad (4)$$

Where σ[S/m] is the electrical conductivity, $\vec{E}$ is the electric field [V/m], and $\vec{J_e}$ is he external current density [A/m²].

$$\vec{E} = \nabla V - \frac{\partial A}{\partial t} \qquad (5)$$

Where V [V] is the electric potential

$$\nabla \times \vec{E} = -\frac{\partial \vec{B}}{\partial t} \qquad (6)$$

The relationship between magnetic field of a metal workpiece and temperature is given by:

$$F = qvBsin\theta \qquad (7)$$

Where F[N] gives the magnetic field produced and q[C] is charge of the material particles. v[m/s] indicates velocity of the material particles being heated. B[T] is the magnetic field and θ is the angle between particle velocity and magnetic field vectors in degrees.

The relationship between temperature and resistance of the workpiece to be heated, is defined as

$$R = R_{ref}[1 + \alpha(T - T_{ref})] \qquad (8)$$

Where R[Ω] gives the material resistance at T temperature and R_{ref}[Ω] is the material resistance at a reference temperature (20°C). α[ppm/°C] is the temperature coefficient of resistance for the material. T[°C] and T_{ref}[°C] are the material temperature and reference temperature that α is specified at.

By controlling the frequency of the Alternating Current, the system can achieve resonance with the inductive and capacitive elements in the circuit. This resonance condition, maximizes the efficiency of energy transfer from the coil to the material being heated.

The resonance circuit typically consists of the induction coil (inductor), a capacitor, and sometimes a matching network to adjust the impedance of the circuit for optimal power transfer.

At the resonance frequency, the reactance of the inductor cancels out the reactance of the capacitor, resulting in the circuit's impedance being solely determined by the resistance. This condition leads to the maximum flow of current through the circuit. Mathematically, the resonance frequency (f_{res}) of an LC circuit can be calculated using the formula:

$$f_{res} = \frac{1}{2\pi\sqrt{LC}} \qquad (9)$$

Where f_{res} [Hz] is the resonance frequency, L[H] is the inductance and C[F] is the capacitance of the resonance circuit.

The relationship between frequency change and workpiece temperature is complex and depends on various factors such as the heating method, frequency range, material properties, and desired heating characteristics.

To describe the Frequency and Heating Rate Generally, higher frequencies result in shallower penetration depths but higher heating rates near the surface. Lower frequencies lead to deeper penetration but slower heating rates. As the frequency changes, the distribution of heat within the workpiece changes accordingly.The heating rate depends on various factors including the power

supplied, material properties, frequency, and geometry of the material being heated. A simplified formula for heating rate in induction heating is:

$$Q = I^2 R \qquad (10)$$

Where Q[J/s] is the heating rate. I[A] is the RMS (Root Mean Square) current flowing through the material and R[Ω] is the resistance of the material.

3.2. Geometry Sequence
Nowadays, a variety of analytical solutions exist to study electromagnetic problems, however, as De Sousa et al. (2014) and Bermúdez et al.(2007) mention 2D electromagnetic processes are still the quickest and also most efficient if Finite Element Method codes are employed to solve the forward problem. The paper illustrates the two-dimensional axisymmetric geometry of the model under consideration and imported into COMSOL as depicted in Figure 3. The coil includes 8 turns and the radius and width of the workpiece are 15 cm and 0.5 cm, respectively. The specific dimensions of the elements are explicitly outlined in Figure 3.
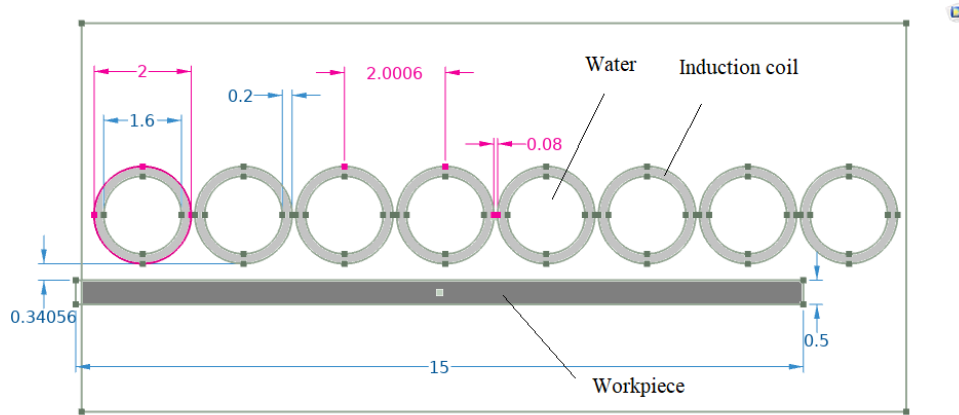

Figure 3. The two-dimensional axisymmetric geometry of the simulation model

3.3. Mesh Sequence
This model uses the transient analysis, induction heating, and electromagnetic interaction modes defined in the AC/DC module of software. The magnetic vector potential is solved in the induction heating simulation using the time-harmonic application mode of quasi-static induction currents (azimuthal induction currents in 2D) Istardi & Triwinarko, (2011). For the infinite element domain user controlled mapped mesh is defined to increase the effectiveness. After that, the number of layers of a domain is selected. Since the excitation current frequency is almost high, the skin effect is inevitable. The skin depth is evaluated by the theoretical knowledge. Later, the thickness and size of layers are added. As receding from the surface of the material, the layers' thickness gets wider. Figure 4 displays the mesh created for the model. A dense mesh is applied especially to the surface of the workpiece and coil to obtain a proper calculation of electromagnetic phenomena. The maximum element size, minimum element size, maximum element growth, and curvature factor are defined as 0.148 cm, 5E-4 cm, 1.25, and 0.25, respectively.
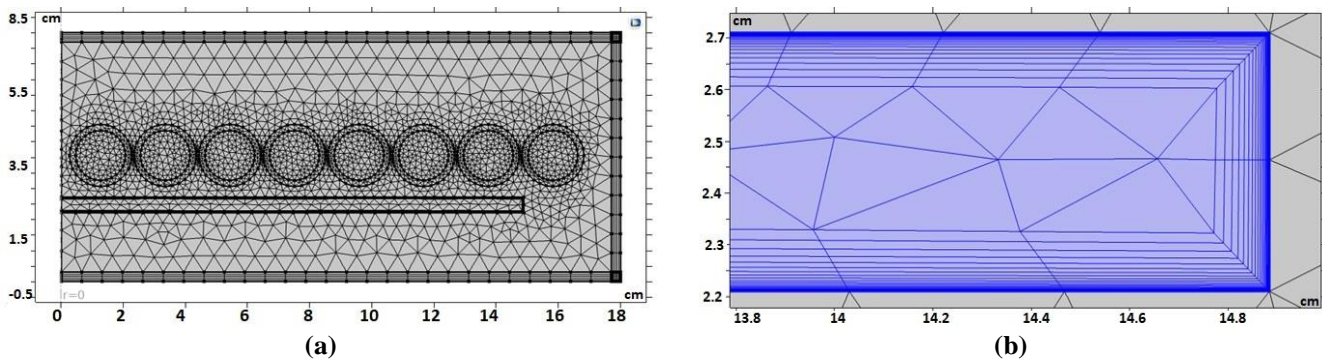

(a)

(b)

Figure 4. The mesh quality of designed model by using finite Element method: (a) designed model's mesh, (b) surface layers of the workpiece

3.4. Physical Model

In electromagnetic simulation computations, the magnetic insulation boundary barrier when the magnetic field disappears must be defined. As mentioned, the induction coil's possible diameter in this work is 34 cm, whereas the workpiece includes a radius of 15 cm. So, a boundary geometry with 36 cm diameter and 8 cm height is sufficient to be defined as the magnetic insulation boundary. The inductor is defined as being cooled by water flowing in a coiled tube. The convective heat transfer coefficient is determined as 16.5 W/(m²·K) by default. The copper tube's water loop has an isothermal constraint fixed at 20°C. Table 1 displays the properties of the materials utilized in the model.

Table 1. Properties of simulation materials

Material	Copper[23]	Aluminum	Water
Relative permittivity	1	1	1
Electrical conductivity [S/m]	5.998e7	3.774e7	5.5e-6
Relative permeability	1	1	80
Thermal conductivity [W/(m·K)]	400	238	Default
Constant pressure heat capacity at [J / (Kg·K)]	385	900	Default
Density [Kg/m³]	8700	2700	Default
Reference resistivity [Ω·m]	1.754e-8	9.7e-8	Default
Resistivity temperature coefficient [1/K]	0.0039	0.0039	Default

4. Simulation Results

4.1. Frequency Domain Analysis

The simulation process for the designed induction heating coil and workpiece interaction is presented in this section. As previously stated, the simulation study comprises two stages. The initial scenario is achieved by investigating the heating process for the current flowing through the induction coil in frequency domain analysis and evaluating the parameters in various frequencies. Modeling the heat transfer problem yields the latter case, in the time domain (frequency transient study) by evaluating the heating process and temperature change for a specified current and frequency.

4.1.1. Frequency variation

In the AC/DC module, the frequency domain analysis is utilized instead of the preset transient analysis to perform the induction heating. In this step, the induction coil power, coil resistance, skin depth and inductance quantities have been evaluated for five different frequencies, and the results are presented in Table 2.

Table 2. Coil power, coil resistance, skin depth and inductance with frequency variation

Frequency [Hz]	Induction Coil Power [W]	Coil Resistance [mΩ]	Skin Depth (δ) [mm]	Inductance [μH]
500	206.75	8.9032	3.67	0.758
5000	98.774	10.133	1.166	0.476
20000	68.636	17.173	0.580	0.308
30000	33.984	22.608	0.473	0.296
60000	28.542	39.756	0.335	0.284

Since the skin effect depends on frequency, it is clear that with higher frequencies the skin depth decreases gradually and the electromagnetic field penetration into the workpiece gets weaker. In addition, the current density rises near the material boundary. As depicted in Figure 5, a specific point is assigned in the workpiece as point 70, and the distribution of the current density norm (J) at this point (point 70) with an increment in frequency is calculated and the result plot is given in Figure 6. It is evident from the graph that the current density also increases as the frequency raises.
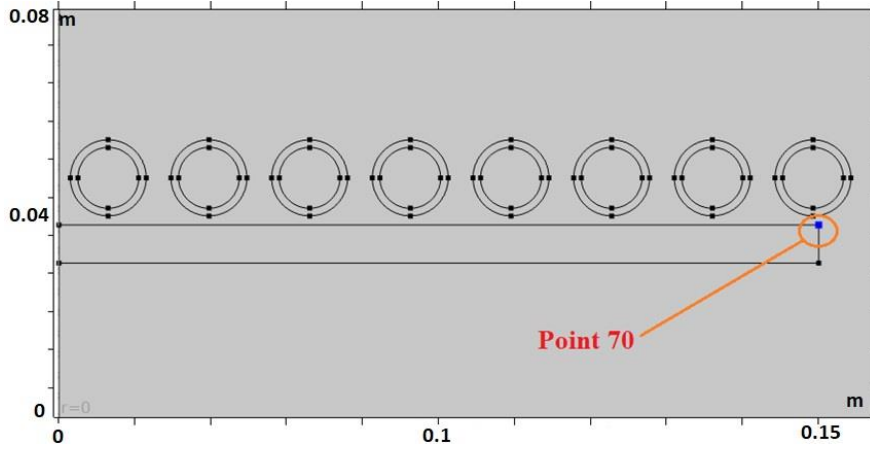
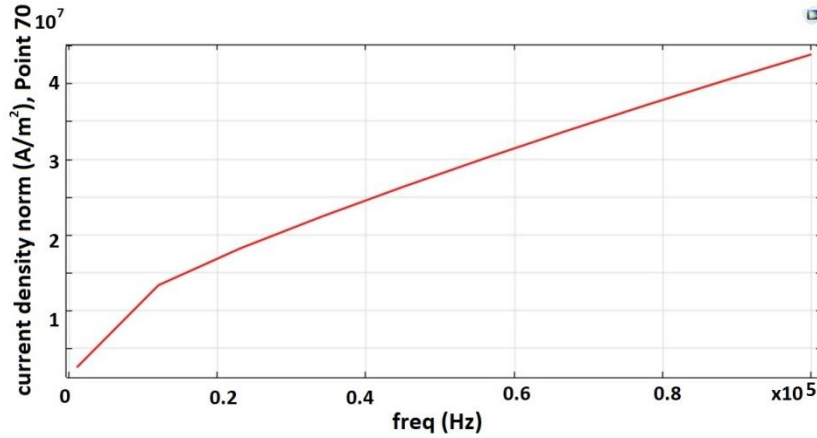**Figure 5**. Assigned point on the workpiece

Figure 6. Current density norm (J) increase with increasing frequency

The coil's power dissipation for various frequencies is also calculated and plotted in Figure 7.
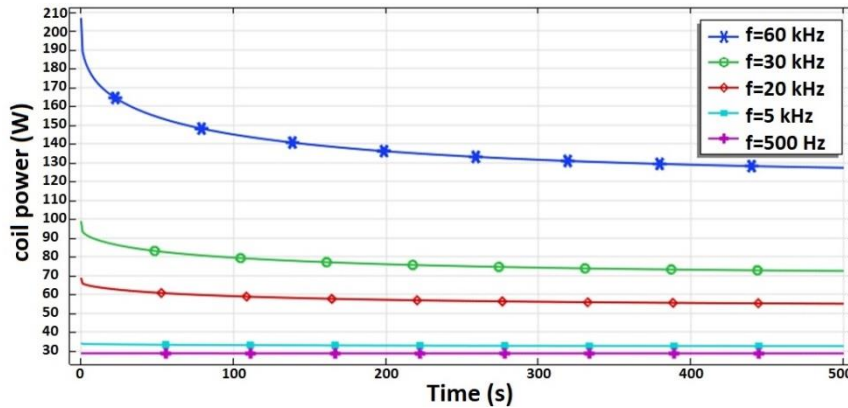

Figure 7. The power dissipation on the coil for various frequencies

It can be inferred that with increasing the frequencies The power dissipation on the coil increases with increasing frequency and this quantity for each frequency differs from the other concerning time.

The effects of frequency on magnetic flux density for a coil current of 10 A and various frequencies at point 70 are shown in Figure 8. According to the plot as the frequency increases The magnetic flux density distribution rises and reaches its maximum for the highest frequency.
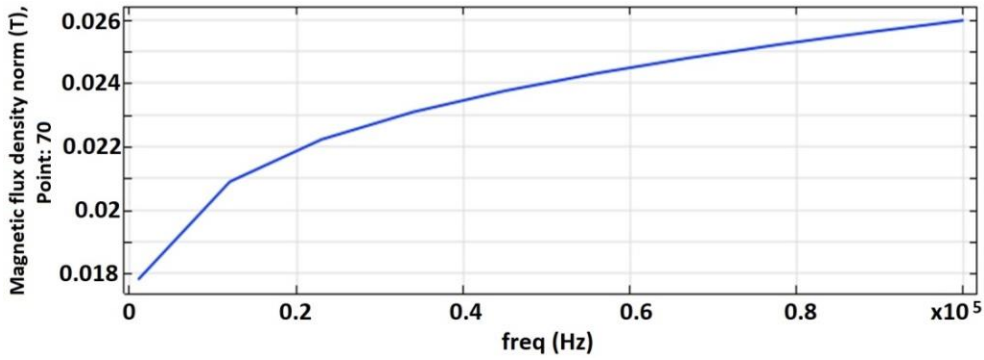
Figure 8. Distribution of magnetic flux density at different frequency and same current of 10 A.

4.1.2. Heat transfer

In the study, the temperature distributions obtained at the end of 500 seconds when a steady current of 10A at 500Hz, 5 kHz, 20 kHz, 30 kHz, and 60 kHz frequencies flow through the coil are shown in Figure 9. The maximum temperature is reached at the highest current frequency (60 kHz) to 780°.
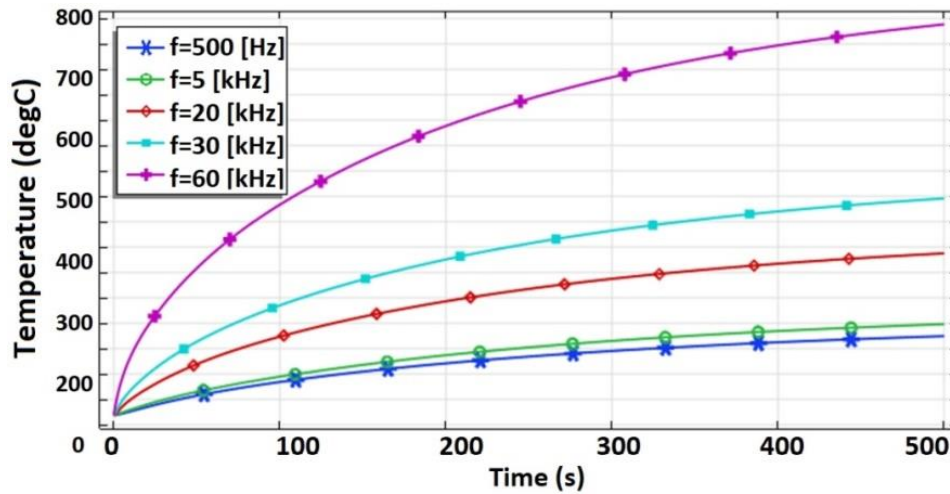

Figure 9. The temperature pattern acquired after 500 seconds for various frequencies

4.2. Frequency Transient Analysis

This section aims to model the heat transfer problem in the time domain. However, since the input signal (excitation current) of the model is sinusoidal, it is possible to model the magnetic field's problem in the frequency domain and this information can be transferred to the heat transfer physics, which can be solved using the time-dependent solver. Hence, to enhance the speed of analysis, the 'Frequency Transient' study is used. The analysis of the induction heating process is performed with a 10 A current and a constant frequency of 10 kHz and the magnetic flux density norm, the temperature variation, the isothermal contours, the skin effect, and magnetic flux distribution are investigated. The Magnetic Flux Density Norm for Revolved Geometry (mf) is given in Figure 10. The distribution of magnetic field flux is almost uniform and homogeneous, as the coil's physics is defined as homogeneous multi-turn and since the coil type is Archimedean spiral the concentration of current in the middle side is higher and it can be observed in Figure 10.c. Additionally, the concentration of flux in the coil increases over time and it is plotted by global evaluation of derived values in Figure 11.
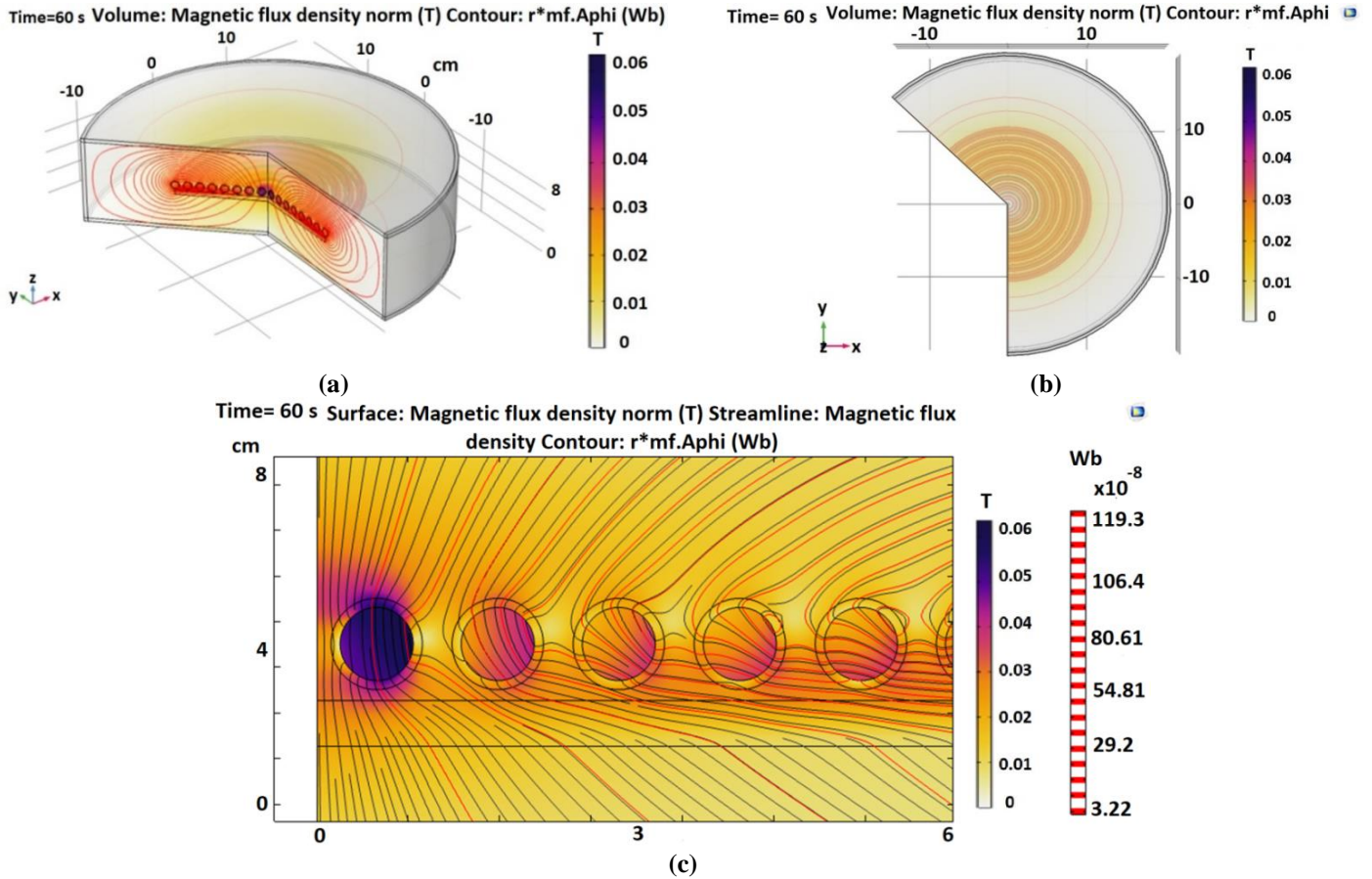
(a)

(b)

(c)

Figure 10. Magnetic Flux Density Norm for Revolved Geometry (mf): (a) 3D xOyOz plane coordinates, (b) xOy plane coordinated, (c) 2D surface view
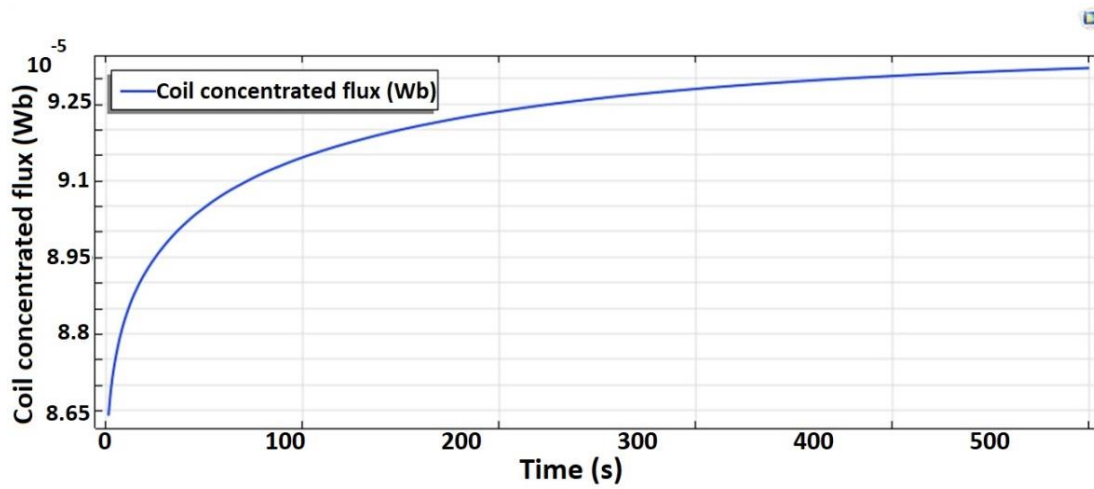

Figure 11. The coil concentrated flux

The temperature rise on the coil and hence on the workpiece are depicted by iso-thermal contours in induction heating physics for t=0 s (as the current starts flowing), t=3 s, t=20 s, and t=60 s as depicted in Figure 12.
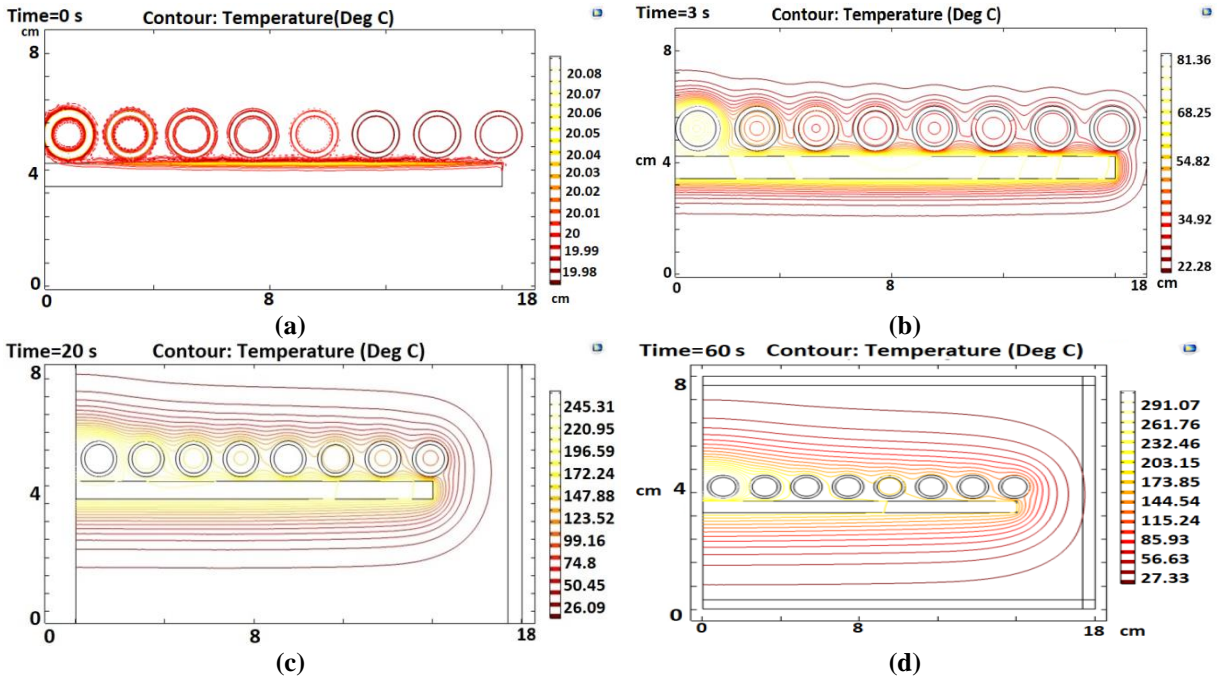
Figure 12. Iso-thermal contours in induction heating physics for; (a) t=0 s, (b) t=3 s, (c) t=20 s and (d) t=60 s

It can be deduced from the iso-thermal analysis contour lines that the temperature increases with the same current and frequency for passing time. The heating process and the temperature variation are visualized in Figure 13.
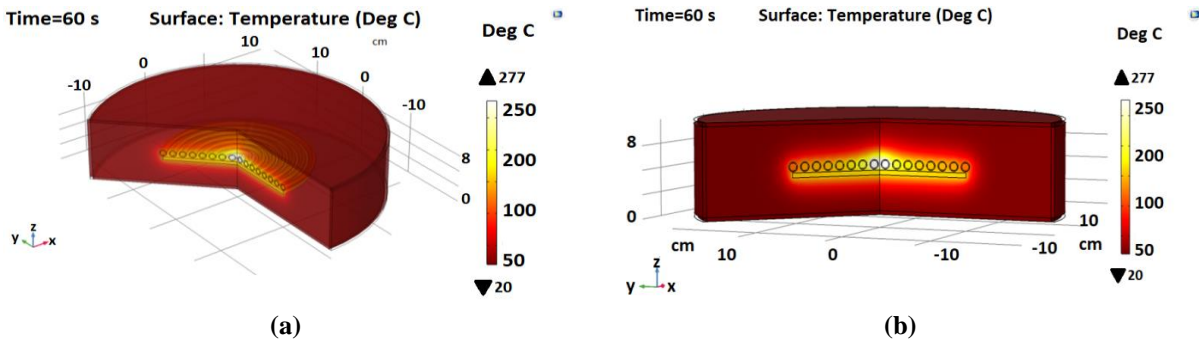

Figure 13. The temperature variation at the end of 60s: (a) xOyOz coordinates, (b) yOz coordinates
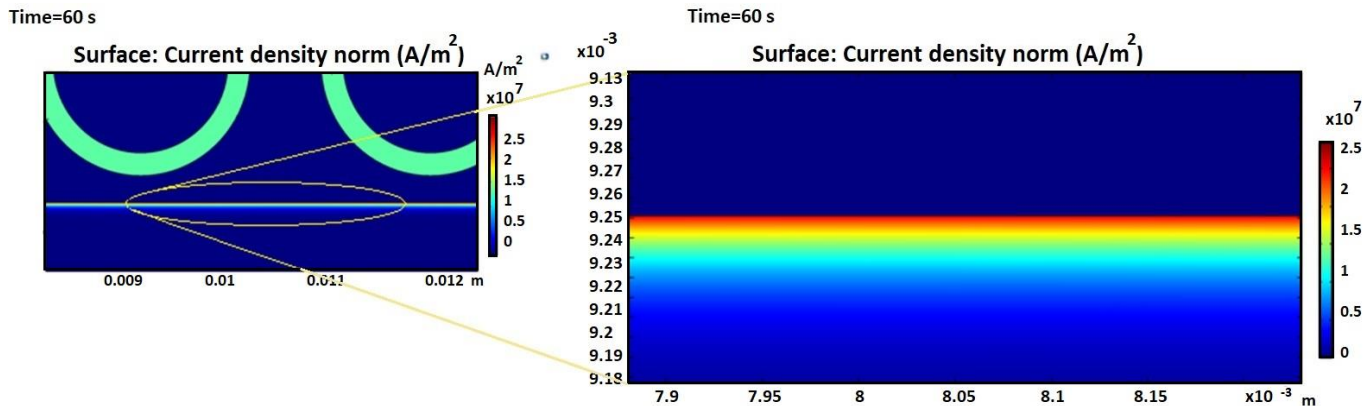

Figure 14. The skin depth of the workpiece with 10 A, 10 kHz excitation

The coil of the model is defined as a homogeneous multi-turn coil and includes no eddy currents. Hence, the skin effect of the coil is neglected. Nevertheless, the skin effect on the workpiece (Aluminum) is depicted in Figure 14 for 10 A and 10 kHz excitation current. It is obvious that because of the kHz range of the frequency, the current tends to flow on the surface of the material and as the color legend indicates, the current depth drops with receding from the surface to the center.

5. Experimental Results

The experimental setup of the induction heating system is constructed and the performance of the designed system is tested as shown in Figure 15. The pancake-shaped coil shown in Figure 16 is used to establish the resonance circuit and the coil parameters are presented in Table 3.

Table 3. Induction coil parameters

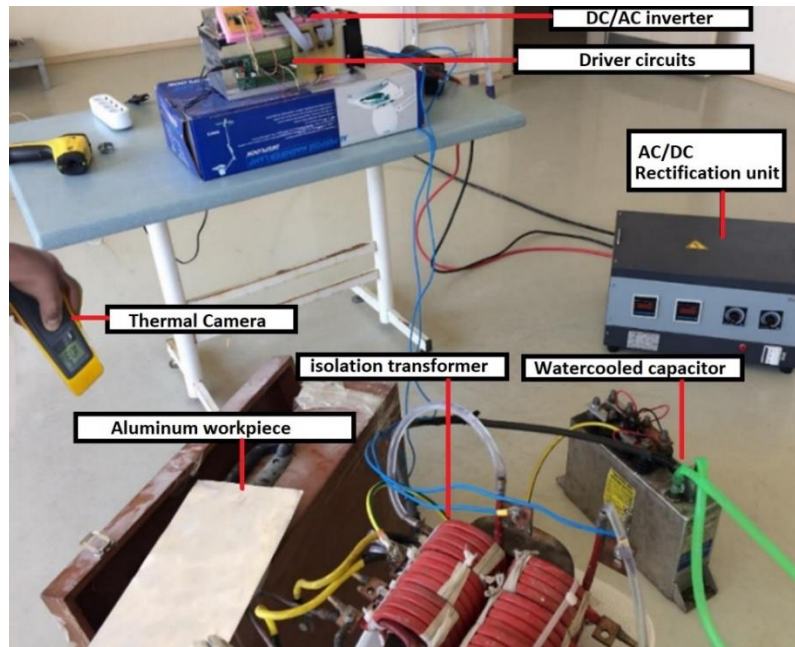| Material type	Copper
Dielectric type	Hard silicon
No. of turns	8
Coil Diameter [cm]	20
Inductance [µH]	3

Figure 15. The experimental setup of designed induction heating system

To prepare the practical setup of the system, an inverter is needed to be employed as stated in Section 2. The characteristics of the prototype inverter (switch types, etc.), the power supply quantities, and the resonant circuit elements used in the experimental setup are presented in Table 4.

Table 4. The parameters of experimental setup

Device	Model/Value
Power supply (including the rectifier)	500V DC, 50A DC out, 400 V AC, 50 Hz, 3-phase
IGBT switches	SKM 150 GB 12T4
IGBT drivers	DA 102D2 IGBT LMY
DSP card	TMS 320F 8335
Resonance inductor [µH]	3
Resonance capacitor [µF]	45
Operating frequency [kHz]	13.3
Aluminum workpiece dimensions[mm]	280*180*2

Figure 16. The pancake shaped (spiral) coil used in experimental study

Figure 17. Measuring the temperature of the workpiece over time

The measurements are performed under resonance conditions with an excitation current of 15A at 13.3 kHz. The Aluminum workpiece is exposed close to the induction coil as presented in Figure 17, and the transferred heat is measured by FLUKE-61 infrared thermal camera (Figure 18). The results are examined over time and illustrated in Table 5. It is clear that as the time passes the temperature of the workpiece increases.
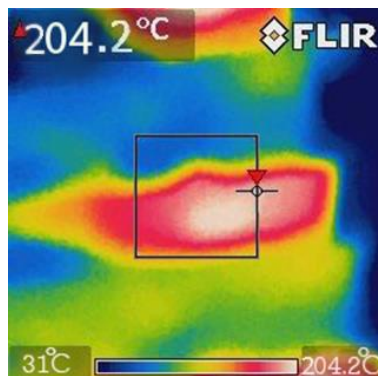

Figure 18. Measured workpiece temperature by the thermal camera

Table 5. The temperature rise in workpiece over time

Time (s)	Temperature(°C)
30	42
50	50
65	92
85	107
100	125
115	140
125	157
145	178
155	195
170	204

6. Conclusion

This paper presents the design of an induction heating system featuring an Archimedean spiral coil intended for heating metals in various industrial applications. The mathematical calculations and simulation of the system have been carried out. In addition, the results for experimental measurements have been obtained The conclusion drawn from both simulation and experimental studies suggests that, for an excitation current with a constant frequency, the heating process is achieved to a satisfactory degree. The simulation results indicate that with rising the excitation current frequency, due to the increase in magnetic flux density generated around the coil, the induction heating process exhibits a better performance. However, in a real induction heating system, the operating frequency is defined as the resonance frequency for efficient energy transfer, and thus, this frequency is selected as the most suitable for the system. Furthermore, in practice, an increase in the excitation current must be limited due to the cable's capacity for carrying current. Hence, it is quite normal for the system to function at a specific frequency and a limited maximum current for efficient performance Future work could involve developing various models of the heating coil using magnetic modeling software, with the potential to enhance the efficiency of induction heating systems. Moreover, research can be conducted on additional functionality, such as overheating protection, overcurrent protection, overvoltage protection, power control, etc. for induction heating devices.

Acknowledgement

References

Aflyatunov, R. R., Khazieva, R. T., & Vasilyev, P.I. (2022). Development and research of an induction heating system for a long pipeline. *Journal of Physics*: Conference Series, 2182(1). IOP Publishing. Doi: 10.1088/1742-6596/2182/1/012039

Aydemir, M. T., Zafarmand, F., Uslu, A., Ünver, H. M., Baranoğlu, B., & Aydın, E. (2019). Design and Implementation of an Induction Heating System for Brittle Sheet Metals. *International Journal of Natural and Engineering Sciences*, 11(3), 29–33. Retrieved from https://ijnes.org/index.php/ijnes/article/view/300

Baranoğlu, B., Özbek, M. E., & Aydın, E. (2020). İndüksiyon ön ısıtmalı bir elektromanyetik darbe şekillendirme sisteminin deneysel analizi. *Gazi Üniversitesi Mühendislik Mimarlık Fakültesi Dergisi* C, 35(4), 2101-2112, Doi:10.17341/gazimmfd.605773

Bermúdez, A., Gómez, D., Muñiz, M.C., & Salgado, P. (2007). Transient numerical simulation of a thermo electrical problem in cylindrical induction heating furnaces. *Advances in Computational Mathematics* 26: 39–62. Doi: 10.1007/s10444-005-7470-9

Bocharova, O., Tynchenko, Vadim., Bocharov, A., Oreshenko, T., Murygin, A., & Panfilov, I. (2019). Induction heating simulation of the waveguide assembly elements. Journal of Physics: Conference Series. 1353. 012040. Doi 10.1088/1742-6596/1353/1/012040

Dalaee, M., Gloor, L., Leinenbach, Ch., & Wegener, K. (2019) Experimental and numerical study of the influence of induction heating process on build rates Induction Heating-assisted laser Direct Metal Deposition (IH-DMD). *Surface and Coatings Technology* 384: 125275. Doi: 10.1016/j.surfcoat.2019.125275

De Sousa, W.T.B., Polasek, A., Dias, R., C.F.T, M., & De Andrade, R. (2014). Thermal–electrical analogy for simulations of superconducting fault current limiters. *Cryogenics* 62: 97-109. Doi: 10.1016/j.cryogenics.2014.04.015

Dou, Q. (2022). Summary of Research on Electromagnetic Induction Heating Temperature Control Method under the Background of Internet Convergence. 2022 4th International Conference on Inventive Research in Computing Applications (ICIRCA), Coimbatore, India, pp. 38-41, Doi: 10.1109/ICIRCA54612.2022.9985648

Esteve, V., Jordan, J., Sanchis, E., Dede, E.J., Maset, E., Ejea, J.B., & Ferreres, A. (2015). Enhanced Pulse-Density-Modulated Power Control for High Frequency Induction Heating Inverters. *IEEE Transactions on Industrial Electronics.* 62. 1-1. Doi: 10.1109/TIE.2015.2436352

Gholami, M., Verougstraete, B., Vanoudenhoven, R., Baron, G.V., Van Assche, T., & Denayer, J. F.M. (2022). Induction heating as an alternative electrified heating method for carbon capture process. *Chemical Engineering Journal* 431(4), 1385-8947. Doi: 10.1016/j.cej.2021.133380

Istardi, D., & Triwinarko, A. (2011). Induction Heating Process Design Using COMSOL® Multiphysics Software, ISSN: 1693-6930, *Telkomnika*, 9(2), August, pp. 327-334. Doi:10.12928/telkomnika.v9i2.704

Jinkun, M., Guangyu, Zh., Yidan, Y., & Jingquan, L. (2021). COMSOL Simulation for Design of Induction Heating System in VULCAN Facility. *Science and Technology of Nuclear Installations*, Article ID 9922503, 12 pages, Doi: 10.1155/2021/9922503

Kennedy M. W., Akhtar, S., Bakken, J. A., & Aune R. E. (2011). Analytical and Experimental validation of electromagnetic simulations using COMSOL re Inductance induction heating and magnetic field, Comsol Conference, Stuttgart, Germany

Kennedy, M., Akhtar, S., & Bakken, J., & Aune, R. (2011). Analytical and Experimental Validation of Electromagnetic Simulations Using COMSOL®, re Inductance, Induction Heating and Magnetic Fields. COMSOL users' conference, Stuttgart, Germany

Liu H, Rao J (2009). Coupled modeling of electromagnetic-thermal problem in induction heating process considering material operties. In 2009 International Conference on Information Engineering and Computer Science (pp. 1-4). IEEE

Ludtke, U., & Schulze, D. (2001). FEM software for simulation of heating by internal sources, Proc. of HIS-01 Int. Seminar, Padua, Italy, Sept. 12-14.

Miyake, D., Umetani, K., Kawahara, S., Ishihara, M., & Hiraki, E. (2022) High-Efficiency Solenoid Coil Structure for Induction Heating of Cylindrical Heating Object. 2022 IEEE 31st International Symposium on Industrial Electronics (ISIE), Anchorage, AK, USA, 307-313, Doi: 10.1109/ISIE51582.2022.9831459

Najafi, E., & Yatim, A. H. (2011). Design and implementation of a new multilevel inverter topology. *IEEE transactions on industrial electronics* 59(11): 4148-4154. Doi:10.1109/TIE.2011.2176691

Qu, H.P., Lang, Y.P., Yao, C.F., Chen, H.T., & Yang, C.Q. (2013). The effect of heat treatment on recrystallized microstructure, precipitation and ductility of hot rolled Fe-Cr-Al-REM ferritic stainless steel sheets, *Materials Science and Engineering*: A, 562, 9-16. Doi: 10.1016/j.msea.2012.11.008

Sankar, S., Ajith, G., & Ramesan, M. T. (2022). Copper alumina@ poly (aniline-co-indole) nanocomposites: synthesis, characterization, electrical properties and gas sensing applications. *RSC advances* 12(27): 17637-17644. Doi: 10.1039/D2RA02213C

Segura, G. M (2012). Induction Heating Converter's Design, Control and Modelling Applied to Continuous Wire Heating, Doctoral Dissertation, Universitat Politecnica de Catalunya, Barcelona, Spain

Waluyo, Ratna, S., & Kurniadi, M. R. (2022). Induction Heating Stove Prototype of 130 kHz using Arduino Uno. In Electrotehnica, *Electronica, Automatica (EEA)* 70(1), 39-50, ISSN 1582-5175. Doi: 10.46904/eea.22.70.1.1108005

Xiaolong, W., Hui, Y., Guangliang, L., & Zhao, Z. (2011). The application of COMSOL multiphysics in direct current method forward modeling. *Procedia Earth and Planetary Science* 3: 266-272. Doi: 10.1016/j.proeps.2011.09.093